Journal of the Korean Nuclear Society
Volume 27, Number 2, April 1995

An Improved Heat Transfer Prediction Model for Turbulent Falling Liquid Films with or Without Interfacial Shear

Seok Jeong Park and Moon Hyun Chun
Korea Advanced Institute of Science and Technology
(Received September 9, 1994)

계면 전단응력이 있을 때와 없을 때 하강하는 난류액막에 대한 개선된 열전달 예측 모델

박석정 · 전문헌
한국과학기술원
(1994. 9. 9 접수)

Abstract

An improved method is presented for the prediction of heat transfer coefficients in turbulent falling liquid films with or without interfacial shear for both heating or condensation. A modified Mudawwar and El-Masri's semi-empirical turbulence model, particularly to extend its use for the turbulent falling film with high interfacial shear, is used to replace the eddy viscosity model incorporated in the unified approach proposed by Yih and Liu. The liquid film thickness and asymptotic heat transfer coefficients against the film Reynolds number for wide range of interfacial shear predicted by both present and existing methods are compared with experimental data. The results show that, in general, predictions of the modified model agree more closely with experimental data than that of existing models.

요 약

계면 전단응력이 있을 때와 없을 때 가열 또는 응축되면서 하강하는 난류액막의 열전달 계수를 예측하기 위한 개선된 방법을 제시하였다. 특히 큰 계면 전단응력이 있을 때 하강하는 난류액막에 적용할 수 있도록 Mudawwar와 El-Masri의 준 실험적 난류모델을 수정하여 Yih와 Liu가 제안한 통합적 접근방법에 사용한 와류점성모델대신에 사용하였다. 광범위한 크기의 계면전단응력에 대해 액막 레이놀즈 수 대 액체막 두께 및 접근적 열전달 계수를 개선된 방법과 다른 여러 기존 방법으로 예측하여 실험값들과 비교하였다. 그 결과 일반적으로 수정한 모델과 예측한 값이 다른 기존 모델로 예측한 값보다 실험치와 더 밀접하게 일치하는 것을 보여주었다.

1. Introduction

Since the pioneering work of Nusselt laminar film flow model [1], a large number of theoretical and experimental studies have been reported concerning the prediction of heat transfer rates accompanying

the phenomena of laminar and turbulent falling films undergoing condensation, evaporation, heating, and cooling. Based on the underlying assumptions used, the existing models for heat transfer in falling liquid films can be broadly classified into (1) laminar film flow models and (2) turbulent film flow models.

The majority of earlier theoretical analyses subsequent to that of Nusselt have attempted to relax one or more of the simplifying assumptions included in the Nusselt's analysis. Rohsenow [2], for example, considered the effects of subcooling in the condensate film and nonlinear temperature distributions. Modeling of turbulent liquid films has been also the target of extensive research spanning over the last six decades. For the analysis of heat transfer in turbulent falling liquid films with or without interfacial shear, an appropriate turbulence model for ε_M and ε_H in the liquid film is required to compute the velocity profile and the Nusselt number. In more recent years, modeling efforts for prediction of heat transfer in falling liquid films have been concentrated on the turbulence model to determine the eddy-viscosity profile across the film. This fact can be clearly observed in the excellent summaries of important turbulence models for prediction of heat transfer in falling liquid films given in recent papers by Yih and Liu [3] and Mudawwar and El-Masri [4]. In these summaries alone, there are at least 14 different turbulence models including their own models.

Existing turbulent film flow models can be further classified based on (1) whether or not the interfacial shear has been included in the model and (2) the criterion used for film flow regime. Essentially two criteria are used to characterize the film flow regime viz.: the film Reynolds number (Re_Γ) and the dimensionless film thickness (δ^+). Film Reynolds numbers (Re_Γ) ranging from 240 to 2100 have been proposed for the laminar to turbulent flow transition. Similarly the values of the dimensionless film thickness (δ^+) at which turbulent mixing within the film is initiated are reported to vary between 6 and 22 [5]. From the above brief review of existing models, following questions may arise immediately:

(1) Which turbulence model is the most reliable for predictions of heat transfer in turbulent falling liquid films ? What are the effects of the interfacial shear and how do these different turbulence models affect the predictions of heat transfer in the given problem ?

(2) What are the reasonable values for the film flow transition criteria ?

The present work has been initiated to address the above questions. In addition, in an effort to improve the most current general approach and to examine the effects of turbulence models and the interfacial shear on the heat transfer in turbulent falling liquid films following approaches are used here : First, Yih and Liu's unified approach [3] has been selected and modified by replacing their turbulence model with a modified Mudawwar and El-Masri's [4] semi-empirical turbulent-film model. Secondly, the effects of turbulence models and the interfacial shear on the heat transfer have been examined by comparing various quantities (e.g., h_x^* and δ^*) for different values of the dimensionless interfacial shear stress (τ_i^*) and film Reynolds number (Re_Γ) obtained by both Yih and Liu's original method [3] and the present modified method along with other existing models.

2. Theory Based on the Most Current Works

In an effort to improve the applicability and the accuracy of the best existing general approach for the present problem as well as to examine the effects of various turbulence models on the final result of the heat transfer in turbulent falling liquid films, the authors have partly modified Yih and Liu's [3] unified procedure. That is, a new semi-empirical turbulent-film model proposed by Mudawwar and El-Masri [4] has been slightly modified first to include the effect of interfacial shear. Then, the modified semi-empirical turbulence model is substituted for the Yih and Liu's [3] turbulence model. A brief outline of the modifications made in the present work is given here

along with Yih and Liu's [3] derivations of the unified procedure for the prediction of average film thickness and local heat transfer coefficients in turbulent film heating, evaporation or condensation with or without interfacial shear.

2.1. Basic Physical Model

As shown in Fig. 1, the basic physical model considered is a vertical flat plate where heating, condensation or evaporation occurs at constant wall heat flux. For example, if the temperature of the wall is below the saturation temperature, condensation occurs on the wall and a liquid film is formed. Over the upper part of the wall, the condensate film flows down the wall in essentially laminar flow under the influence of the gravity and the interfacial shear associated with the condensing vapor. Over the lower part of the wall, however, the flow within the layer changes from laminar to turbulent when the condensation rate is sufficiently high or a sufficient thickness is attained. In this analysis for turbulent falling liquid films, most of the Nusselt's assumptions are retained : (1) The liquid film is fully developed and has a smooth surface, (2) flow acceleration and momentum changes are neglected, and (3) all physical properties are assumed constant. In Fig. 1, some of the basic quantities that occur in the analysis are shown.

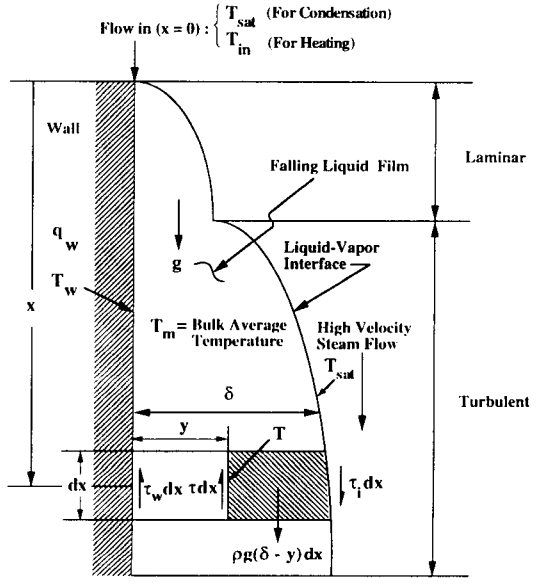

Fig. 1. Physical Model for Falling Turbulent Liquid Films with Interfacial Shear

2.2. Governing Equations

Heat and momentum are simultaneously transferred through the liquid film at rates which are dependent upon the nature and thickness of the condensate film. Therefore, the solution of the present problem requires a relation between the thickness of the layer and the distance along the wall and a specification of the thermal resistance of the layer. These quantities can be obtained from a simultaneous solution of the following simplified partial differential equations of momentum and energy for the liquid film :

$$\tau = \rho(\nu + \varepsilon_M)\frac{du}{dy} \tag{1}$$

$$u\frac{\partial T}{\partial x} = \frac{\partial}{\partial y}(\alpha + \varepsilon_H)\frac{\partial T}{\partial y} \tag{2}$$

Note that the shear stress is expressed in terms of the velocity gradient. From the force balance of a liquid element, the local shear stress distribution in the liquid film and the wall shear can be obtained as

$$\tau = \rho(\delta - y)g + \tau_i \tag{3}$$

$$\tau_w = \rho g\delta + \tau_i \tag{4}$$

Dimensionless variables and quantities are defined as follows :

$$\delta^* = \delta\left(\frac{g}{\nu^2}\right)^{1/3};\ \delta^+ = \frac{u^*\delta}{\nu};\ u^* = \left(\frac{\tau_w}{\rho}\right)^{1/2}$$

$$\tau_i^* = \frac{\tau_i}{\rho(\nu g)^{2/3}};\ s^3 = \frac{\rho g\delta}{\tau_i + \rho g\delta};\ u^+ = \frac{u}{u^*}$$

$$x^+ = \frac{u^* x}{\nu \mathrm{Pr}};\ y^+ = \frac{u^* y}{\nu} \tag{5}$$

Then, following relations can be obtained :

$$s^3 + \frac{\tau_i^* s^2}{\delta^{+2/3}} - 1 = 0$$

$$\delta^* = s\delta^{+2/3}$$

$$\frac{\tau}{\tau_w} = 1 - \frac{s^3 y^+}{\delta^+} \tag{6}$$

Using above quantities, Eqs. (1) and (2) can be represented in dimensionless form as

$$\frac{du^+}{dy^+} = \frac{\frac{\tau}{\tau_w}}{1+\frac{\varepsilon_M}{\nu}} = \frac{1-\frac{s^3 y^+}{\delta^+}}{1+\frac{\varepsilon_M}{\nu}} \tag{7}$$

$$u^+ \frac{\partial \theta}{\partial x^+} = \frac{\partial}{\partial y^+}\left[(1+\frac{\mathrm{Pr}}{\mathrm{Pr}_T}\frac{\varepsilon_M}{\nu})\frac{\partial \theta}{\partial y^+}\right] \tag{8}$$

where $\mathrm{Pr}_T = \frac{\varepsilon_M}{\varepsilon_H}$ and θ is a dimensionless temperature defined by

$$\theta = \frac{T - T_{in}}{q_w \delta / k} \quad \text{(for heating at constant wall heat flux)} \tag{9}$$

and

$$\theta = \frac{T - T_{sat}}{q_w \delta / k} \quad \text{(for evaporation or condensation at constant wall heat flux)} \tag{10}$$

It should be noted here that if $\tau_i = 0$, $s^3 = 1$ and the above equations reduce to the nonsheared film case. The film Reynolds number can be obtained from

$$Re_\Gamma = \frac{4\Gamma}{\mu} = 4\int_0^{\delta^+} u^+ dy^+ \tag{11}$$

2.3. Heating at Constant Wall Heat Flux

Applicable boundary conditions for the energy equation, Eq. (8), are

$$\theta = \theta_{in}(y^+) \quad \text{at } x^+ = 0 \text{ (inlet)} \tag{12}$$

$$\frac{\partial \theta}{\partial y^+} = -\frac{1}{\delta^+} \text{ (constant wall heat flux)}$$

$$\text{at } y^+ = 0 \text{ (wall)} \tag{13}$$

$$\frac{\partial \theta}{\partial y^+} = 0 \text{ (Zero interfacial heat flux)}$$

$$\text{at } y^+ = \delta^+ \text{ (liquid-vapor interface)} \tag{14}$$

When both velocity and temperature profiles are fully developed,

$$\frac{\partial \theta}{\partial x^+} = \frac{d\theta_m}{dx^+} = \frac{d\theta_w}{dx^+} = constant \tag{15}$$

where θ_m and θ_w are the dimensionless temperatures corresponding to the bulk average temperature (T_m), and the wall temperature (T_w), respectively.

Equation (15) shows that θ is of the following form :

$$\theta = C_1 x^+ + F(y^+) \tag{16}$$

Substituting Eq. (16) into Eq. (8)

$$C_1 u^+ = \frac{d}{dy^+}\left[(1+\frac{\mathrm{Pr}}{\mathrm{Pr}_T}\frac{\varepsilon_M}{\nu})\frac{dF}{dy^+}\right] \tag{17}$$

Equation (17) can be integrated using the boundary conditions, Eqs. (13) and (14) and $\varepsilon_M = 0$ at $y^+ = 0$ to obtain

$$F(y^+) = C_1 \int_0^{y^+} \frac{\int_0^{y^+} u^+ dy^+ - \frac{Re_\Gamma}{4}}{1+\frac{\mathrm{Pr}}{\mathrm{Pr}_T}\frac{\varepsilon_M}{\nu}} dy^+ \tag{18}$$

where $C_1 = \frac{4}{\mathrm{Re}_\Gamma \delta^+}$. Thus, Eq. (8) has been integrated to give

$$\theta = \theta_w + \frac{4}{Re_\Gamma \delta^+}\int_0^{y^+} \frac{\int_0^{y^+} u^+ dy^+ - \frac{Re_\Gamma}{4}}{1+\frac{\mathrm{Pr}}{\mathrm{Pr}_T}\frac{\varepsilon_M}{\nu}} dy^+ \tag{19}$$

where $\theta_w = \frac{4x^+}{Re_\Gamma \delta^+}$

The dimensionless bulk average temperature θ_m is also found as

$$\theta_m = \frac{\int_0^{\delta^+} u^+ \theta dy^+}{\int_0^{\delta^+} u^+ dy^+} = \theta_w + \frac{16}{Re_\Gamma^2 \delta^+}$$

$$\left[\int_0^{\delta^+} u^+ \left(\int_0^{y^+} \frac{\int_0^{y^+} u^+ dy^+ - \frac{Re_\Gamma}{4}}{1+\frac{\mathrm{Pr}}{\mathrm{Pr}_T}\frac{\varepsilon_M}{\nu}} dy^+ \right) dy^+ \right] \tag{20}$$

The heat transfer coefficient for heating at constant wall heat flux is defined as $h_x = q_w/(T_w - T_m)$ and the Nusselt number can be derived as

$$Nu_x = \frac{1}{\theta_w - \theta_m} =$$

$$\left[\frac{16}{Re_\Gamma^2 \delta^+} \int_0^{\delta^+} u^+ \left(\int_0^{y^+} \frac{\frac{Re_\Gamma}{4} - \int_0^{y^+} u^+ dy^+}{1 + \frac{Pr}{Pr_T}\frac{\varepsilon_M}{\nu}} dy^+ \right) dy^+ \right]^{-1} \quad (21)$$

The dimensionless local heat transfer coefficient h_x^* is related to Nu_x by

$$h_x^* = \frac{h_x}{k}\left(\frac{\nu^2}{g}\right)^{1/3} = \frac{Nu_x}{s\,\delta^{+2/3}} \quad (22)$$

2.4. Condensation (or Evaporation) at Constant Wall Heat Flux

The energy equation, Eq. (8) is still applicable but θ is now defined by Eq. (10). The heat transfer coefficient for the present case is defined as $h_x = q_w/(T_w - T_{sat})$. Applicable boundary conditions are :

$$\theta = 0 \ (T = T_{sat}) \qquad \text{at } x^+ = 0 \quad (23)$$

$$\frac{\partial \theta}{\partial y^+} = -\frac{1}{\delta^+} \text{(constant wall heat flux)}$$

$$\text{at } y^+ = 0 \text{ (wall)} \quad (24)$$

$$\theta = 0 \ (T = T_{sat}) \quad \text{at } y^+ = \delta^+ \text{ (liquid-vapor interface)} \quad (25)$$

Under fully developed conditions, $\frac{\partial \theta}{\partial x^+} = 0$. Equation (8) can be integrated applying the boundary conditions, Eqs. (24) and (25) and $\varepsilon_M = 0$ at y^+ to obtain

$$\theta = \frac{1}{\delta^+} \int_{y^+}^{\delta^+} \frac{1}{1 + \frac{Pr}{Pr_T}\frac{\varepsilon_M}{\nu}} dy^+ \quad (26)$$

The local Nusselt number and the dimensionless local heat transfer coefficient can also be derived as

$$Nu_x = \frac{1}{\theta_w} = \frac{\delta^+}{\int_0^{\delta^+} \frac{1}{1 + \frac{Pr}{Pr_T}\frac{\varepsilon_M}{\nu}} dy^+} \quad (27)$$

$$h_x^* = \frac{h_x}{k}\left(\frac{\nu^2}{g}\right)^{1/3} = \frac{Nu_x}{s\,\delta^{+2/3}} \quad (28)$$

It should be noted here that the above results are obtained for the boundary condition of constant wall heat flux. However, as noted by Yih and Liu [3], the resulting asymptotic Nusselt number should apply equally well to the boundary condition of constant wall temperature because, for turbulent flow with Prandtl numbers greater than unity, there is essentially no difference between the two cases.

2.5. Modified Turbulence Model

Details of five turbulence models including the present model are given in Table 1. Comparisons of the various existing models show that the semi-empirical turbulent-film model offered by Mudawwar and El-Masri [4] seems to have the least arbitrariness in the sense that their model is largely based on the well known experimental data. However, the interfacial shear has not been considered in the Mudawwar and El-Masri [4] turbulence model. In the flow condensation of steam inside tubes, in particular, the shear force acting on the condensation film by the high velocity steam has an important effect on the flow state of condensate film and the heat transfer coefficient. Therefore, present authors modified their model to include the effects of interfacial shear τ_i and to be consistent with Eqs. (3) and(4).

When τ_i is included, the eddy viscosity profile in the bulk region obtained by Mudawwar and El-Masri [4] from the experimental profile of Ueda et al. [8] can be written as

$$\frac{\varepsilon_M}{\nu} = l^{+2}\frac{du^+}{dy^+} = Ky^+\left(\frac{\tau}{\tau_w}\right) = Ky^+\left(1 - \frac{s^3 y^+}{\delta^+}\right) \quad (29)$$

For $\frac{\varepsilon_M}{\nu} \gg 1$, Eq. (29) can be combined with Eq. (7)

Table 1. Important Turbulence Models of Falling Liquid Films with interfacial Shear

Authors	Process	Model	
Rohsenow, Webber & Ling [6]	Condensation with Interfacial Shear	$0 \le y^+ \le 5$ $5 \le y^+ \le 30$ $30 \le y^+$	$\frac{\varepsilon_M}{\nu} = 0$ $\frac{\varepsilon_M}{\nu} = \frac{y^+}{5} - 1$ $\frac{\varepsilon_M}{\nu} = \frac{y^+}{2.5}$, $Pr_T = 1.0$
Hubbard et al. [7]	Condensation, Evaporation with Interfacial Shear	$0 \le y^+ \le y_i^+$ $y_i^+ < y^+ \le \delta^+$	$\frac{\varepsilon_M}{\nu} = -\frac{1}{2} + \frac{1}{2}\sqrt{1 + 4K^2 y^{+2}(\tau/\tau_w)\left[1 - \exp(-y^+/A^+)\right]^2}$ $\frac{\varepsilon_M}{\nu} = \frac{8.13\times10^{-17}(\nu g)^{2/3}}{Ka\, u^{*2}} Re_\Gamma^{2n}\left[1 + b(\tau_i/\tau_w^o)\right]^2(\delta^+ - y^+)^2$ $Pr_T = 0.9, 1.0, 1.1$, $K = 0.4$, $A^+ = 26$, $n = 6.95\times10^2\,\nu^{1/2}$, $b = 0.9 + 1.73\times10^{12}\,\nu^2$, ν in m^2/sec
Yih & Liu [3]	Condensation, Evaporation with Heating with Interfacial Shear	$0 \le y^+ \le 0.6\delta^+$ $0.6\delta^+ < y^+$	$\frac{\varepsilon_M}{\nu} = -\frac{1}{2} + \frac{1}{2}\sqrt{1 + 4K^2 y^{+2}(\tau/\tau_w)\left\{1 - \exp\left[-y^+(\tau/\tau_w)^{1/2}/A^+\right]\right\}^2 \exp\left[-1.66(1 - \tau/\tau_w)\right]^2}$ $\frac{\varepsilon_M}{\nu} = \frac{\varepsilon_M}{\nu}\Big\|_{y^+ = 0.6\delta^+}$, $Pr_T = \frac{1 - \exp\left[-y^+(\tau/\tau_w)^{1/2}/A^+\right]}{1 - \exp\left[-y^+(\tau/\tau_w)^{1/2}/B^+\right]}$ $\tau/\tau_w = 1 - s^3 y^+/\delta^+$, $K = 0.4$, $A^+ = 25.1$, $B^+ = f(Pr)$
Mudawwar & El-Masri [4]	Evaporation and Heating for Freely Falling Film	$0 \le y^+ \le \delta^+$	$\frac{\varepsilon_M}{\nu} = -\frac{1}{2} + \frac{1}{2}\sqrt{1 + 4K^2 y^{+2}(\tau/\tau_w)^2\left\{1 - \exp\left[-y^+(\tau/\tau_w)^{1/2}/A^+\left(1 - 0.865(Re_\Gamma)_{crit}^{o\,1/2}/\delta^+\right)\right]\right\}^2}$ $\tau/\tau_w = 1 - y^+/\delta^+$, for heating : $(Re_\Gamma)_{crit}^o = 97/Ka^{0.1}$, for evaporation : $(Re_\Gamma)_{crit}^o = 0.04/Ka^{0.37}$ $Pr_T = 1.4\exp(-15\, y^+/\delta^+) + 0.66$, $K = 0.4$, $A^+ = 26$
Present	Condensation, Evaporation and Heating with Interfacial Shear	$0 \le y^+ \le \delta^+$	$\frac{\varepsilon_M}{\nu} = -\frac{1}{2} + \frac{1}{2}\sqrt{1 + 4K^2 y^{+2}(\tau/\tau_w)^2\left\{1 - \exp\left[-y^+(\tau/\tau_w)^{1/2}/A^+(1 - \delta_{crit}^+/\delta^+)\right]\right\}^2}$ $\tau/\tau_w = 1 - s^3 y^+/\delta^+$, $\delta_{crit}^+ = \frac{1}{s^{3/2}}\left\{\left[3/4\,(Re_\Gamma)_{crit}^o\right]^{1/3} - \tau_i^*\right\}^{3/2}$ (for low τ_i^*) or 21 (for high τ_i^*) $Pr_T = 1$, for heating: $(Re_\Gamma)_{crit}^o = 97/Ka^{0.1}$, for condensation: $(Re_\Gamma)_{crit}^o = 0.04/Ka^{0.37}$, $K = 0.4$, $A^+ = 26$

to obtain the mixing length profile

$$l^+ = \frac{u^* l}{\nu} = Ky^+(1 - \frac{s^3 y^+}{\delta^+})^{1/2} \quad (30)$$

The viscous sublayer is accounted for by introducing the Van Driest [9] damping function D to the turbulent mixing length as follows :

$$l^+ = Ky^+ D(1 - \frac{s^3 y^+}{\delta^+})^{1/2} \quad (31)$$

Substituting Eq.(31) into Eq.(29) for l^+

$$\frac{\varepsilon_M}{\nu} = K^2 y^{+2} D^2 (1 - \frac{s^3 y^+}{\delta^+}) \frac{du^+}{dy^+} \quad (32)$$

The above equations, therefore, are applicable throughout the liquid layer. Combining these equations with Eq. (7), the following eddy-viscosity distribution function is obtained :

$$\frac{\varepsilon_M}{\nu} = -\frac{1}{2} + \frac{1}{2}\left[1 + 4K^2 y^{+2}(1 - \frac{s^3 y^+}{\delta^+})^2 D^2 \right]^{1/2} \quad (33)$$

Similarly, by incorporating τ_i, the Van Driest damping function has been modified as

$$D = 1 - \exp\left[-\frac{y^+}{26}(1 - \frac{s^3 y^+}{\delta^+})^{1/2} X_{lam} \right] \quad (34)$$

The laminarization parameter X_{lam} in Eq.(34) can be written as [4]

$$X_{lam} = 1 - \frac{\delta^+_{crit}}{\delta^+} \quad (35)$$

Equation (35) suggests that as δ^+ approaches its critical value (δ^+_{crit}), X_{lam} will approach zero, and the flow will become completely laminar.

2.6. Transition Criteria for Laminar to Turbulent Film

Two dimensionless critical film thickness (δ^+_{crit}) as criteria for transition from laminar to turbulent film flow are chosen here, i.e., one for low τ_i^* (e.g., $\tau_i^* < 4.5$ for heating or condensation at 100°C) and the other for high τ_i^* (e.g., $4.5 \le \tau_i^* \le 300$ for heating or condensation at 100°C). The criterion for low τ_i^* values is derived first. For a laminar film flow, $\varepsilon_M = 0$, and the following expression can be obtained from Eq. (7):

$$u^+ = y^+ - \frac{1}{2}(\frac{\delta^*}{\delta^+})^3 y^{+2} \quad (36)$$

Substituting Eq. (36) into Eq. (11) and using the relations given in Eq. (6) and integrating

$$Re_\Gamma = \frac{4}{3}\delta^{*3} + 2\tau_i^* \delta^{*2} \quad (37)$$

For the special case of $\tau_i^* = 0$, an expression for δ_{crit} can be obtained in terms of $(Re_\Gamma)^o_{crit}$ from Eq. (37) :

$$\delta_{crit} = \left[\frac{3}{4}(Re_\Gamma)^o_{crit} \frac{\nu^2}{g} \right]^{1/3} \quad (\text{for } \tau_i^* = 0) \quad (38)$$

where $(Rep)^o_{crit}$ is defined as the critical film Reynolds number for transition from laminar to turbulent film when $\tau_i^* = 0$.

Also, the expression for $(\tau_w)_{crit}$ when $\tau_i^* \neq 0$ can be obtained by using Eq. (38) in Eq. (4) [6] :

$$(\tau_w)_{crit} = \rho g \left[\frac{3}{4}(Re_\Gamma)^o_{crit} \frac{\nu^2}{g} \right]^{1/3} \quad (39)$$

Equating the right hand sides of Eqs. (4) and (39)

$$\rho g \delta_{crit} + \tau_i = \rho g \left[\frac{3}{4}(Re_\Gamma)^o_{crit} \frac{\nu^2}{g} \right]^{1/3} \quad (40)$$

Using Eqs. (5) and (6) the above equation can be rewritten as

$$\delta^+_{crit} = \frac{1}{s^{3/2}}\left\{ \left[\frac{3}{4}(Re_\Gamma)^o_{crit} \right]^{1/3} - \tau_i^* \right\}^{3/2} \quad (41)$$

However, the transition condition given by Eq. (41) has only a limited applicability to the region of low values of τ_i^* because it requires (δ^+_{crit}) to be negative when $\tau_i^* > \frac{3}{4}\left[(Re_\Gamma)^o_{crit} \right]^{1/3}$

For freely-falling turbulent liquid films, Mudawwar and El-Masri [4] correlated the $(Re_\Gamma)^o_{crit}$ from existing data for heated or isothermal films and also for evaporating films as follows :

$$(Re_\Gamma)^o_{crit} = \frac{97}{Ka^{0.1}} \quad (\text{for heating}) \quad (42)$$

$$(Re_\Gamma)^o_{crit} = \frac{0.04}{Ka^{0.37}} \quad (\text{for evaporation}) \quad (43)$$

In the above equations, $(Re_\Gamma)^o_{crit}$ is treated as a fun-

ction of Kapitza number defined by $Ka \equiv \frac{\mu^4 g}{\rho \sigma^3}$. As a result of using the assumptions (2) and (3), $(Re_\Gamma)^0_{crit}$ becomes the same for both evaporation and condensation. Therefore, Eq. (43) is also applicable to the case of condensation.

Another criterion is necessary for high interfacial shear condensation and/or evaporation. For very high values of τ_i^* it is possible that δ^+_{crit} approaches a limiting value. The critical Reynolds number and the critical dimensionless film thickness (δ^+_{crit}) suggested by various workers are shown in Table 2 for the case of high interfacial shear. Based on the result of high interfacial shear condensation data (i.e., the range of τ_i^* values is from 10 to 300), Ueda et al. [12] obtained the following limit condition of laminar flow:

$$\delta^+_{crit} = \frac{\delta_{crit}}{\nu}\left(\frac{\tau_w}{\rho}\right)^{1/2} = 21 \tag{44}$$

It is recommended here to use the δ^+_{crit} value calculated by Eq. (44) if δ^+_{crit} value computed from Eq. (41) is less than that from Eq. (44).

Now, combining Eqs. (33), (34), and (35) the complete eddy-viscosity profile can be expressed as

$$\frac{\varepsilon_M}{\nu} = -\frac{1}{2} + \frac{1}{2}\sqrt{1 + 4K^2 y^{+2}\left(1 - \frac{s^3 y^+}{\delta^+}\right)^2\left\{1 - \exp\left[-\frac{y^+}{26}\left(1 - \frac{s^3 y^+}{\delta^+}\right)^{1/2}\left(1 - \frac{\delta^+_{crit}}{\delta^+}\right)\right]\right\}^2} \tag{45}$$

In the above equation, K is von Karman's constant (K=0.40) and δ^+_{crit} is given by either Eq. (41) (for low τ_i^*) or Eq. (44) (for high τ_i^*). The $(Re_\Gamma)^0_{crit}$ in Eq.(41), on the other hand, is given by Eq. (42) or Eq. (43) depending on whether the liquid film is under heating condition or evaporation (and/or condensation).

3. Calculation Method

The original problem is to obtain the Nusselt number by simultaneously solving Eqs. (7) and (8) with a set of boundary conditions given for heating or condensation at constant wall heat flux. However, since Eq. (8) has already been integrated to obtain the expressions for the Nusselt number, it can be replaced by Eq. (21) or Eq. (27).

The first process in finding Nu_x is to express u^+ as a function of y^+ which is equivalent to the integration of Eq. (7). To integrate Eq. (7), following steps are required:

1) First select a typical value of τ_i^* and a value of δ^+, substitute these values into the first expression of Eqs. (6) and solve for s.
2) δ^+_{crit} can be calculated from Eqs. (41) and (44).
3) Using δ^+_{crit} and s, the quantity $\frac{\varepsilon_M}{\nu}$ can be obtained from Eq. (45).
4) $\frac{\varepsilon_M}{\nu}$ and s are then substituted into Eq. (7) and the velocity profile, $u^+(y^+)$, is obtained by any numerical method of integration (such as a Gaussian quadrature or a fourth-order Runge-Kutta method).

The film Reynolds number Re_Γ defined by Eq. (11) is also obtained by integrating the velocity profile using a Gaussian quadrature. In this manner one can obtain a plot of δ^* vs. Re_Γ for different values

Table 2. Critical Reynolds Number and Dimensionless Critical Film Thickness for Liquid Film Flow with High Interfacial Shear Proposed by Previous Workers

Authors	$(Re)_{crit}$ or δ^+_{crit}	Methods Used
Carpenter and Colburn [10]	$(Re)_{crit}=240$	Experiment
Rohsenow et al. [6]	$\delta^+_{crit}=6$, $(Re)_{crit}=71.8$	Analysis
Ueda, Akiyoshi et al. [11]	$\delta^+_{crit}=22$, $(Re)_{crit}=970$	Experiment
Ueda, Kubo and Inoue [12]	$\delta^+_{crit}=21$, $(Re)_{crit}=800-900$	Experiment
Lilburne and Wood [5]	$\delta^+_{crit}=12.5$	Analysis
Present Work	$\delta^+_{crit}=21$	Analysis

of τ_i^+ (e.g., Figs. 3 and 4) since $\delta^* = s\delta^{+2/3}$.

The Nusselt number (Nu_x) or the dimensionless local heat transfer coefficient (h_x^+), on the other hand, can be evaluated in a manner similar to the above procedure :

Equations (41), (44), and (45) are used to evaluate $\frac{\varepsilon_M}{\nu}$ and the above results for δ^+, Re_Γ and $u^+(y^+)$ are substituted into Eq. (21) or Eq. (27) to calculate Nu_x. The dimensionless local heat transfer coefficient h_x^+ can then be found from Eq. (22) or Eq. (28). In this manner, a series of h_x^+ values as a function of Re_ρ for different values of τ_i^+ (e.g., Figs. 5, 6, and 7) can be calculated.

The turbulent Prandtl number (Pr_T) in Eqs. (21) and (27) can be larger than 1 near the wall but approaches 1 as $y^+ \to \delta^+$ [3]. However, there is no reliable conclusion about the turbulent Prandtl number. Therefore, (Pr_T) is assumed to be equal to unity in the present calculation.

The calculation procedure for the case of no interfacial shear (i.e., $\tau_i^+ = 0$ and $s = 1$) is about the same. The base conditions for the present numerical solution are summarized in Table 3.

4. Results and Discussion

4.1. Eddy-Viscosity Distribution

It should be noted here that when $s = 1$ ($\tau_i^+ = 0$) Eq. (29) reduces to the original expression for the variation of eddy viscosity in the bulk region selected by Mudawwar and El-Masri [4] for their proposed turbulence model. The original equation was based on experimental measurements in a free-surface liquid layer. Nevertheless, the present authors have modified to extend its use for liquid film flow with high interfacial shear. The final form of the present eddy-viscosity profile is thus given by Eq. (45).

A comparison between the predictions given by Eq. (45) and some of the existing models is given in Fig. 2. These curves show the eddy-viscosity distributions across a vertical condensate water film at 100 ℃ with and without interfacial shear. From Fig. 2 following observations can be made :

1) All these models tend to converge in the vicinity of the wall.
2) One of the previous models proposed by Hubbard et al. [7] tends to decrease eddy viscosity in the bulk region by a discontinuous function and becomes zero at the liquid-vapor interface.
3) As opposed to the previous model, Eq. (45) gives a continuous linear variation of eddy viscosity and the location of the maximum $\frac{\varepsilon_M}{\nu}$ value tends to move closer to the liquid-vapor interface as τ_i^+ increases from zero to 30.

In the case of open channel flow, in particular, reported by Ueda et al. [8], the measured distribution of eddy diffusivity for momentum has its maximum at $\frac{y}{\delta} = 0.45$ and decreases very rapidly in the outer half region, $\frac{y}{\delta} > 0.45$.

Table 3. The Base Conditions for the Present Numerical Calculations

Conditions for Numerical Calculations (Heating)							
Fluid	T(°C)	P(bar)	ρ(kg/m^3)	μ(N·sec/m^2)	σ(N/m)	Pr	Ka
water	20	1.0133	998.3	1.003×10^{-3}	7.724×10^{-2}	7	2.58×10^{-11}
Conditions for Numerical Calculations (Condensation)							
Fluid	T(°C)	P(bar)	ρ(kg/m^3)	μ(N·sec/m^2)	σ(N/m)	Pr	Ka
water	88.7	0.6672	960.0	3.197×10^{-4}	6.107×10^{-2}	2	4.68×10^{-13}
water	100.3	1.0242	957.9	2.813×10^{-4}	5.866×10^{-2}	1.75	3.14×10^{-13}
water	101.4	1.0650	957.1	2.781×10^{-4}	5.865×10^{-2}	1.73	3.04×10^{-13}

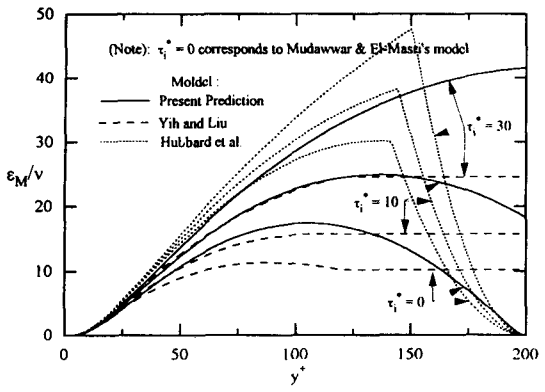

Fig. 2. Comparison of the Modified Turbulence Model with Existing Models for the Eddy-Viscosity Distribution Across a Vertical Condensate Water Film with or without Interfacial Shear (τ_i=0,10 and, 30) at 100°C (δ^+=200)

4.2. Effects of Turbulence Model ($\frac{\varepsilon_M}{\nu}$), τ_i^* and Re_Γ on δ^*

First to assess the effects of turbulence model ($\frac{\varepsilon_M}{\nu}$), intertacial shear ($\tau_i$), and film Reynolds number (Re_Γ) on the predictions of δ^*, δ^* vs. Re_Γ for various τ_i^* values predicted by present model and Yih and Liu's [3] model are compared with experimental data. In Fig. 3, δ^* vs. Re_Γ for various τ_i^* values predicted by two different models and Brauer's equation [13] (for τ_i^*=0 only) are compared with Ueda and Tanaka [14] data for heating of a turbulent falling film with concurrent gas interfacial shear. In Fig. 4, on the other hand, experimental data of the condensate film thickness during condensation of steam inside a tube obtained by Ueda et al. [12] are compared with predictions of two different analytical models.

Regarding the effects of various parameters on δ^*, following observations can be made from Figs. 3 and 4.

1) Effect of Turbulence Model on δ^*:

The difference between the two predictions, one by the present turbulence model and the other by Yih and Liu's [3], becomes larger as τ_i^* increases and as Re_Γ decreases. However, for Re_Γ > 8000 the agreement between the two predictions becomes increasingly close.

2) Effects of τ_i^* and Re_Γ on δ^*:

For a given liquid film Reynolds number Re_Γ, the dimensionless filtm thickness δ^* decreases as τ_i^* increases for both heating and condensation. When Re_Γ=3000, for example, calculated ratio between the δ^* of the falling film with τ_i^*=80 and that of the free falling film (τ_i^*=0), i.e., δ^+ (at τ_i^*=80)/δ^* (at τ_i^*=0) is about 0.42. Also, for a given τ_i^*, δ^* increases as Re_Γ increases for both heating and condensation.

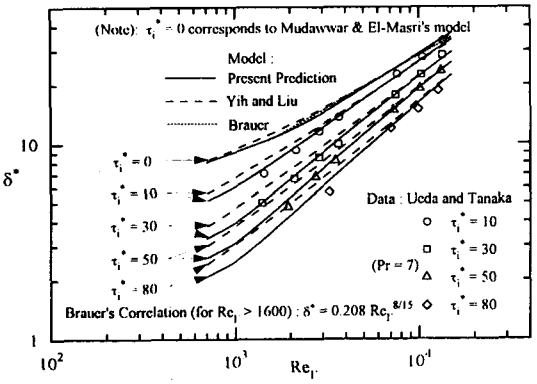

Fig. 3. Predictions of δ^* vs. Re_Γ for Various τ_i^* and Comparison with Data of Ueda and Tanaka [14] for Heating

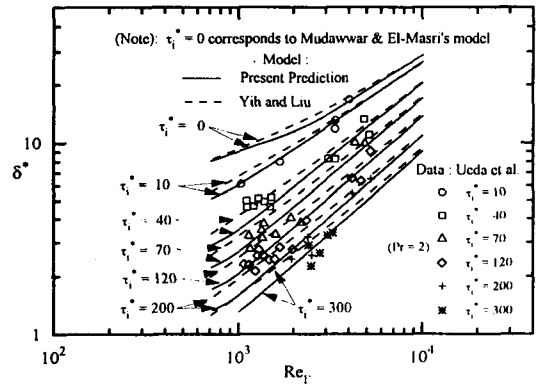

Fig. 4. Predictions of δ^* vs. Re_Γ for Various τ_i^* and Comparison with Data of Ueda, Kubo, and Inoue [12] for Condensation

In general, predictions of the modified model agree more closely with data than that of Yih and Liu's [3] model. Also, for $\tau_i^*=0$, present model agrees closely with the Brauer equation [13] for heating.

4.3. Effects of Turbulence Model ($\frac{\varepsilon_M}{\nu}$), τ_i^* and Re_Γ on h_x^*

To examine the effects of various parameters on the asymptotic dimensionless heat transfer coefficients, h_x^* vs. Re_Γ curves for various τ_i^* are obtained by different models and they are compared with experimental data for heating and condensation.

In Fig. 5, h_x^* vs. Re_Γ curves for four different τ_i^* values (ranging from $\tau_i^*=0$ to $\tau_i^*=100$) predicted by three different models are compared with Ueda and Tanaka [14] data for heating, whereas in Fig. 6, four different model predictions for h_x^* vs. Re_Γ at six different τ_i^* values (from 10 to 300) are compared with the data of Ueda et al. [12] for condensation. In addition, for the special case of low interfacial shear (i.e., $\tau_i^*=1.18$ and $Pr=1.73$), in Fig. 7, four different model predictions for h_x^* vs. Re_Γ are compared with the experimental data for film condensation of steam in concurrent downflow inside a vertical tube reported by Blangetti and Schlünder [15].

From the results shown in Figs. 5, 6, and 7, the effects of various parameters on h_x^* may be briefly summarized as follows:

1) Effect of Turbulence Model on h_x^*:

In the case of heating (Fig. 5), for $Re_\Gamma < 5000$, Yih and Liu's model [3] predicts increasingly larger h_x^* values than the present model as the film Reynolds number is decreased (while τ_i^* varies from 0 to 100), but for $Re_\Gamma > 5000$, the agreement between the two model predictions and the data becomes very close. For condensations, Figs. 6 and 7 show a similar behavior but the film Reynolds number at which two curves (i.e., predicted by the present and the Yih and Liu's models) cross over varies from $Re_\Gamma \cong 4000$ to $Re_\Gamma \cong 6500$ depending on τ_i^* values. All the existing data show that the variation of the heat transfer coefficient with mass flow rate (or equivalently Re_Γ) has a negative slope in laminar regime and a positive slope in turbulent regime. With respect to the slope of h_x^* vs. Re_Γ curves, it should be noted that the curves of the present model shown in Figs. 5, 6, and 7 have positive slopes in turbulent regime while the curves obtained by other models have negative slopes particularly for condensation (Fig. 6).

2) Effects of τ_i^* and Re_Γ on h_x^*:

The asymptotic dimensionless heat transfer coefficient h_x^* increases as τ_i^* is increased for both heating and condensation. Also, for both heating and condensation, h_x^* increases as Re_Γ is increased for a given τ_i^*, but h_x^* is much more dependent on τ_i^* than on Re_Γ at large τ_i^*. This confirms the fact that the interfacial shear exerted by the high velocity steam plays an important role in determining the heat transfer rate in film condensation.

In general, as can be seen in Figs. 5, 6, and 7, agreement between the predictions obtained by the present and Yih and Liu's [3] models tends to become close when $Re_\Gamma > 5000$ (except for $\tau_i^*=0$).

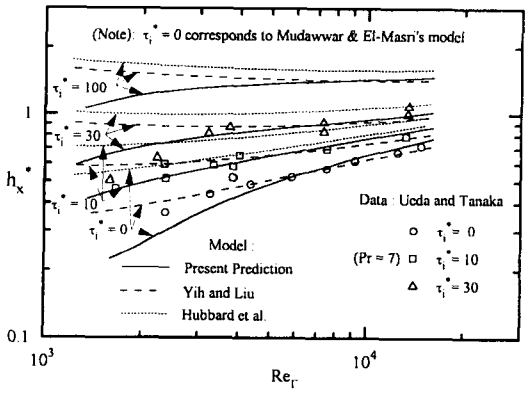

Fig. 5. Predictions of h_x^* vs. Re_Γ for Various τ_i^* and Comparison with Data of Ueda and Tanaka [14] for Heating

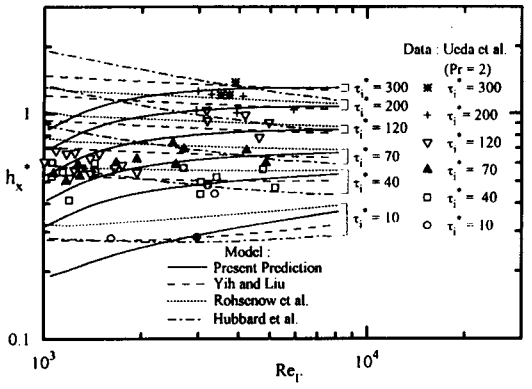

Fig. 6. Predictions of h_x^* vs. Re_f for Various τ_i^* and Comparison with Data of Ueda, Kubo, and Inoue [12] for Condensation

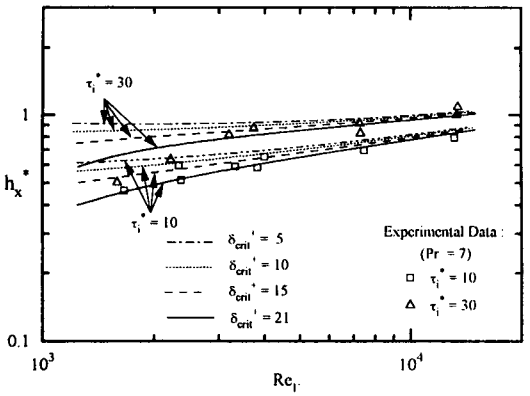

Fig. 8. Predictions of h_x^* vs. Re_f for Various δ_{crit}^+ Values Obtained by Present Model and Comparison with Data of Ueda and Tanaka [14] for Heating

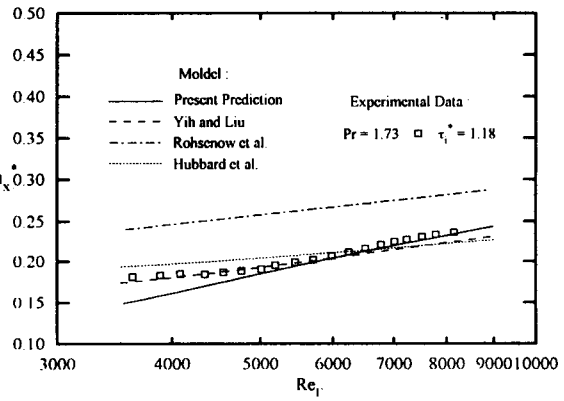

Fig. 7. Predictions of h_x^* vs. Re_f for τ_i^*=1.18 and Comparison with Data of Blangetti and Schlünder [15] for Condensation

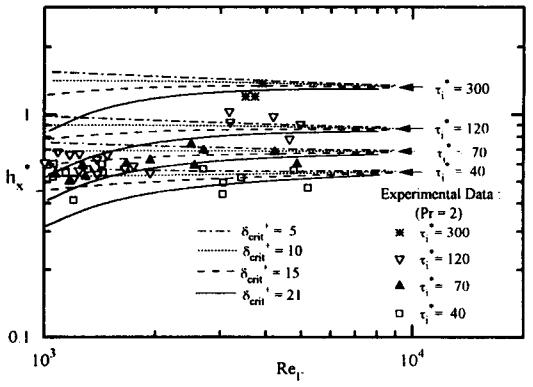

Fig. 9. Predictions of h_x^* vs. Re_f for Various δ_{crit}^+ Values Obtained by Present Model and Comparison with Data of Ueda, Kubo, and Inoue [12] for Condensation

4.4. Effect of δ_{crit}^+ Values for High τ_i^* on h_x^*

For high interfacial shear (e.g., $4.5 \leq \tau_i^* \leq 300$ at 100° C) condensation and/or evaporation, $\delta_{crit}^+ = 21$ has been used in the present model except for low interfacial flow (e.g., $\tau_i^* < 4.5$ at 100°C). However, there is still some uncertainty in choosing the δ_{crit}^+ value for the analysis of film flow under high interfacial shear, because the range of δ_{crit}^+ value proposed by previous workers varies from 6 to 22 as can be seen in Table 2. In addition, except the data of Ueda et al. [11, 12], there are very few reliable data to establish the exact conditions under which transition occurs when there is a significant interfacial shear stress. Therefore, a simple sensitivity study has been performed to examine the effect of δ_{crit}^+ value on the final results of h_x^*. Figures 8 and 9 show a series of h_x^* vs. Re_f curves obtained by present model using four different δ_{crit}^+ values from 5 to 21 for high interfacial shear for heating (Fig. 8) and condensation (Fig. 9). Both figures show that $\delta_{crit}^+ = 21$ gives the best agreement with the data.

5. Conclusions

An improved heat transfer model for turbulent falling liquid film with or without interfacial shear has been derived by using a modified turbulence model of Mudawwar and El-Masri [4], to extend its use for falling films with high interfacial shear in particular, in the unified approach proposed by Yih and Liu [3]. The present modified heat transfer analysis method for turbulent falling liquid film exhibits good agreement with experimental data for wide range of film Reynolds number and dimensionless interfacial shear.

The effects of turbulence model (for $\frac{\varepsilon_M}{\nu}$) and various key film flow parameters, such as τ_i^+, Re_Γ, and δ_{crit}^+, on the heat transfer have also been evaluated with both present and existing models. The results are presented in the form of δ^+ vs. Re_Γ and h_x^+ vs. Re_Γ curves for various τ_i^+ and δ_{crit}^+ values along with experimental data for heating and condensation.

The two criteria for transition from laminar to turbulent film flow, one for low τ_i^+ (e.g., $\tau_i^+ < 4.5$ for heating or condensation at 100°C) and the other for high τ_i^+ (e.g., $4.5 \leq \tau_i^+ \leq 300$ for heating or condensation at 100°C), given by Eqs. (41) and (44), respectively are shown to give the best agreement with the data for the present method.

Acknowledgments

The authors gratefully acknowledge the financial support of the Korea Science and Engineering Foundation through the Center for Advanced Reactor Research at the Department of Nuclear Engineering, KAIST.

Nomenclature

A^+ constant, 25.1 or 26
B^+ Van Driest parameter
C_1 constant used in Eq. (18)
D Van Driest damping function
F quantity used in Eq. (18)
g gravitational acceleration constant
h_x local heat transfer coefficient
k thermal conductivity
K constant, 0.4
Ka Kapitza number, $(\mu^4 g)/(\rho\sigma^3)$
l mixing length
Nu_x local Nusselt number, $h_x\delta/k$
P pressure
Pr Prandtl number
Pr_T turbulent Prandtl number
q_w wall heat flux
Re_Γ film Reynolds number defined by Eq. (11)
s parameter defined by Eq. (5)
T temperature
u liquid film velocity
u* friction velocity defined by Eq. (5)
x distance in flow direction
X_{lam} laminarization parameter defined by Eq. (35)
y distance measured from the wall

Greek

α thermal diffusivity
Γ mass flow rate per unit periphery
δ film thickness
θ dimensionless temperature defined by Eq. (9) or (10)
ε_H eddy diffusivity for heat
ε_M eddy diffusivity for momentum
μ absolute viscosity
ν kinematic viscosity
ρ liquid film density
σ surface tension
τ shear stress

Subscripts

crit critical
i interfacial
in inlet
m bulk average
sat saturation
w wall

Superscripts

+, * dimensionless

o zero interfacial shear

References

1. Nusselt, W., "Die Oberflachen Kondensation des Wasserdampfes," Zeitschrift Verein Deutscher Ingenieure, Vol. 60, 1916, pp. 541−546 and 569−575.
2. Rohsenow, W.M., "Heat Transfer and Temperature Distribution in Laminar Film Condensation," Transactions of the American Society of Mechanical Engineers, Vol. 78, 1956, pp. 1645−1648.
3. Yih, S. M. and Liu, J.L., "Prediction of Heat Transfer in Turbulent Falling Liquid Films with or without Interfacial Shear," AIChE Journal, Vol. 29, No. 6, 1983, pp. 903−909.
4. Mudawwar, I.A. and El-Masri, M.A., "Momentum and Heat Transfer Across Freely-Falling Turbulent Liquid Films," Int. J. Multiphase Flow, Vol. 12, No. 5, 1986, pp. 771−790.
5. Lilburne, G.M. and Wood, D.G., "Condensation inside a Vertical Tube," Proc. 7th Int. Heat Transfer Conf., 1982, pp. 113−118.
6. Rohsenow, W.M., Webber, J.H., and Ling, A.T., "Effect of Vapor Velocity on Laminar and Turbulent-Film Condensation," Trans. ASME, 78, 1956, pp. 1637−1643.
7. Hubbard, G.L., Mills, A.F., and Chung, D.K., "Heat Transfer Across a Turbulent Falling Film with Concurrent Vapor Flow," J. Heat Transfer, Vol. 98, 1976, pp. 319−320.
8. Ueda, H., Möller, R., Komori, S., and Mizushima, T., "Eddy Diffusivity Near the Free Surface of Open Channel Flow," Int. J. Heat Mass Transfer, Vol. 20, 1977, pp. 1127−1136.
9. Van Driest, E.R., "On Turbulent Flow Near a Wall,"J. Aerosp. Sci., Vol. 23, 1956, pp. 1007−1011.
10. Carpenter, E.F. and Colburn, A.P., "The Effect of Vapor Velocity on Condensation Inside Tubes," Proc. of the General Discussion on Heat Transfer, ASME, 1951, pp. 20−26.
11. Ueda, T., Akiyoshi, K., Matsui, T., and Inoue, M., "Heat Transfer and Pressure Drop for Flow Condensation Inside a Vertical Tube," Bull. JSME., Vol. 15, No. 88, 1972, pp. 1267−1277.
12. Ueda, T., Kubo, T., and Inoue, M., "Heat Transfer for Steam Condensing inside a Vertical Tube," Proc. 5th Int. Heat Transfer Conf., Vol. 3, 1974, pp. 304−308.
13. Brauer, H., "Strömung und Wärmeübergang bei Rieselfilmen," VDI-Forschungsheft, 457, 1956.
14. Ueda, T. and Tanaka, T., "Studies of Liquid Film Flow in Two-Phase Annular and Annular-Mist Flow Regions (Part 1, Downflow in a Vertical Tube)," Bull. JSME, Vol. 17, 1974, pp. 603−613.
15. Blangetti, F. and Schlünder, E.U., "Local Heat Transfer Coefficients on Condensation in a Vertical Tube," Proc. 6th Int. Heat Transfer Conf., 2, 1978, pp. 437−442.